

# Co-optimizing transmission and BESS expansions with system strength constraints

Juan Pablo Cerda<sup>a</sup>, Claudia Rahmann<sup>a</sup>, Rodrigo Moreno<sup>a,c,\*</sup>, Luis Morán<sup>b</sup>

<sup>a</sup> Department of Electrical Engineering University of Chile, Santiago, Chile

<sup>b</sup> Department of Electrical Engineering, University of Concepción, Concepción, Chile

<sup>c</sup> Instituto Sistemas Complejos de Ingeniería (ISCI), Santiago, Chile

## ARTICLE INFO

### Keywords:

Converter interfaced generation  
System strength  
System stability  
Transmission expansion planning  
Weak grids

## ABSTRACT

The increased penetration of renewables through converter interfaced generation (CIG) and the associated displacement of synchronous generators (SGs) can significantly reduce system strength. Although some network enhancements, such as the installation of battery energy storage systems (BESS), can partially counterbalance the reduction in strength, current network planning methodologies overlook system strength effects. In this context, this work proposes a new optimization model for co-optimizing investments in network expansions and battery systems to meet, at minimum cost, system strength requirements quantified through short circuit levels (SCL). Recognizing that SCL needs vary on a case-by-case basis, this model incorporates a logistic regression analysis trained on offline time-domain dynamic simulations; this approach effectively correlates SCL with system stability, providing a tailored strategy for each power system. To solve the optimization, we also propose an algorithm to iteratively find the optimal solution for the co-optimized portfolio of new transmission and energy storage investments. Through various case studies, we demonstrate the importance of considering system strength requirements in planning studies with significant penetration of CIG.

## 1. Introduction

### 1.1. Motivation

The energy transition toward low-carbon electricity systems with high shares of converter interfaced generation (CIG), such as photovoltaic and wind generation is already underway. Since 2013, the total worldwide installed capacity of CIG rose from 1567 GW to 3381 GW by the end of 2022 [1]. This energy transition is, however, not an easy task. Significant technical challenges must be first overcome before these newer generation technologies can be widely adopted in bulk electricity systems. Although the challenges cover a wide range of technical issues, several studies and practical experiences have recognized that those related to system stability are among key barriers to overcome, especially under weak grid conditions [2–5].

So far, system robustness against contingencies has largely been ensured by having large amounts of synchronous generators (SGs) distributed throughout the network. During contingencies, these rotating machines naturally provide high short circuit currents and thereby strongly support system stability and recovery after the fault

clearance [4]. Accordingly, strong areas of power systems are usually found close to SGs, while weak areas are far from generation centers [3]. Unlike SGs, the short circuit current contribution from CIG-based power plants is usually limited to values between 1.0 and 1.2 times their rated current due to the thermal limits of power electronics converters [2,6]. These values are significantly lower than the fault current that SGs can provide, which can be up to 6 times their rated current [7,8]. The exact fault current contribution of CIG varies depending on the fault, its duration, and pre-fault operating conditions [6]. The control strategy implemented in the converters also influences the fault current provided by CIG. This way, the displacement of SGs by CIG reduces system strength in the area where the SGs are replaced [2], thereby weakening the power system.

Operational and stability problems in weak power systems with low short circuit levels (SCLs) can manifest themselves in a number of different ways, including classical voltage instability [5], small signal instability [9], and loss of synchronism of conventional machines [10]. During contingencies, these systems may experience extremely depressed voltages over wide network areas, which may challenge voltage recovery after fault clearance and speed up the rotors of the

\* Corresponding author.

E-mail address: [rmorenovieyra@ing.uchile.cl](mailto:rmorenovieyra@ing.uchile.cl) (R. Moreno).

<https://doi.org/10.1016/j.epsr.2024.110696>

Received 1 October 2023; Received in revised form 15 March 2024; Accepted 17 June 2024

Available online 28 June 2024

0378-7796/© 2024 Elsevier B.V. All rights reserved, including those for text and data mining, AI training, and similar technologies.

nearby SGs. New stability phenomena, such as converter-driven instability, control instability and unstable fast control interactions due to dynamic couplings between power electronic converters and the grid, are also most likely to arise under weak grid conditions [2,3,9]. Consequently, the reduction of system strength by increasing CIG can significantly impair the dynamic performance of power systems, thereby making them more prone to instabilities [3,4,5].

The potential solutions to mitigate stability problems in weak networks with high levels of CIG are system specific. The solutions cover a broad spectrum of alternatives including anything from classical network reinforcements to complex changes in the control system of the converters [2,3]. Additional transmission network capacity, line reconductoring, lower impedance transformers, and incorporation of synchronous condensers are all (well-known) corrective measures that can be undertaken to increase SCLs and improve the dynamic behavior of weak systems [11]. Other converter-based devices can also be incorporated in weak network areas to improve system robustness locally [12,13]. For instance, Flexible AC Transmission Systems (FACTS) devices, such as STATCOM and SVCs, as well as Battery Energy Storage Systems (BESS), can help in controlling system voltages through fast reactive current support [12,13]. This helps in limiting voltage fluctuations in steady state and in improving the fault ride-through capability of nearby CIGs [14]. Control changes in CIG power plants and re-tuning of key control parameters can also reduce the risk of instabilities under weak grid conditions [2].

Regardless of the alternative chosen, the mitigation of weak grid conditions for reducing the risk of unstable system responses will always involve additional costs. Still, timely decisions can often avoid the need to adopt hasty and expensive corrective actions—unavoidable once the stability problems have already arisen.

### 1.2. Contributions of this work

Classical transmission network expansion planning (TNEP) tackles the challenge of determining an optimal expansion plan by adding new transmission lines and other network components to serve a growing electricity demand, and/or changes in the generation portfolio. The optimization minimizes the total costs of the system (operational and investment costs) during a study period, subject to a set of technical constraints. Among the technical constraints usually considered are those related to the operational limits of the generation units, load balance, and transmission network capacity.  $N-1$  security constraints are sometimes also included in the optimization, normally by using DC power flow equations [15]. Potential stability issues that may threaten system security are usually assessed in a second stage of the planning process once an optimal expansion plan has been determined. The objective of these studies is to detect hazard situations that may threaten system stability and define suitable corrective measures able to avoid unstable behaviors during critical conditions [16].

While this simple two-stage planning approach has shown to be suitable in robust networks without major stability concerns, it will not be tenable in future electricity systems dominated by CIG. In these cases, several issues such as faster system dynamics, complex control interactions, and unstable behaviors due to weak grid conditions, will push the stability of power systems to their limits. Accordingly, system planners will need to explore enhanced planning approaches in which the underlying stability challenges are somehow considered in the optimization stage. The paradigm shift in energy supply towards electricity systems dominated by CIG will thus require a gradual breakaway from the cornerstones that have sustained power system planning thus far.

In the aforementioned context, in this work we propose a novel optimization model for TNEP considering system strength constraints. The optimization model includes a set of constraints to reduce the probability of unstable behaviors caused by weak grid conditions. The constraints are formulated based on a logistic regression model that exploits the relationship between the SCLs and the dynamic

performance of the system during faults. Specifically, the logistic regression determines the probability of system instability given a SCL. The regression model is trained with detailed offline time-domain dynamic simulations. This unique system strength-constrained optimization problem is solved iteratively by a two-stage algorithm. In the first stage, SCLs are ignored, obtaining a purely economic solution. This solution is then tested in a second stage, where, given the SCLs, the model determines the probability of instability. If this probability is higher than a threshold, we solve again the first stage with an additional constraint that modifies the search space of the first-stage problem, removing previous infeasible solutions. Overall, the model improves short-term voltage and rotor angle stability by increasing the SCLs in weak network areas. For this, additional transmission network capacity, BESS or a combination thereof are considered as investment measures to locally improve the SCLs. BESS are modeled with voltage support capability, so that they can support system stability by injecting reactive current during severe voltage dips.

The remainder of this article is organized as follows: Section II presents a literature review. Section III presents the BESS control model with voltage support capability used in this work. Section IV details the TNEP model by including stability constraint requirements. Section V presents the case study, and Section VI, the results obtained. Finally, Section VII summarizes the conclusions.

## 2. Literature review

### 2.1. BESS in the area of TNEP and system stability

The evaluation of the benefits that BESSs can provide to power systems with CIG is an active research area that has drawn significant attention over the last years. These devices do not only provide the necessary operational flexibility to integrate CIG in electricity systems [17], but also offer significant benefits from a stability standpoint [12].

The fast capability of BESS to inject or consume both active and reactive power allows these devices to support stability during contingencies. The type of support provided depends on the control strategy implemented, as well as on fault type and system operation conditions. Among the several articles harnessing BESS for improving stability, a large majority uses BESS to improve frequency stability through virtual inertia emulation or fast frequency response [18,19]. Still, BESS have also been used to improve rotor angle stability [12,13,20], and voltage stability [21].

Within expansion planning frameworks including BESS, most of published works include these devices to either improve grid congestion management or maximize CIG participation. From these works, it is concluded that the flexibility provided by BESS can reduce system investment costs, especially in the case of high levels of CIG, [22,23]. System operation costs can also be reduced by incorporating different storage devices [22]. The extent of cost reduction will depend on several factors, including market conditions and characteristics pertaining to the system itself (CIG penetration and network distribution). In terms of optimal location, two major trends can be observed: either to locate BESS units nearby CIG-based power plants [17], or in load busbars [23]. Although previous works provide useful outcomes about planning of electricity systems with BESS, planning models considering BESS as a means to improve system strength (and thus stability) have not been put forward thus far.

### 2.2. TNEP considering SCL constraints

Publications about TNEP including SCL or strength constraints are scarce. In [24] and [25], a model based on a Mixed-Integer Linear Programming (MILP) is proposed for co-optimizing transmission and generation expansion. In both works, the SCLs at different busbars are represented using a linearized model. Still, they neglect the short circuit current contribution from new generation units, even though

conventional machines are among the major fault current sources. In [26], the authors propose a short-circuit constrained model for investment decisions at different stages of the planning horizon. The model incorporates detailed representations of voltage levels, alternative bundled conductor options per line, and short circuit limits. However, the proposed model focuses on transmission lines without considering generators or other devices that may also contribute to short-circuit currents.

The research summarized above provides useful insights and results about TNEP considering SCL constraints. However, these planning models solely require a minimum threshold for SCLs without considering its relationship with system stability. Moreover, none of them consider BESS as a network reinforcement alternative to improve SCLs and thereby reduce the probability of unstable behaviors due to weak grid conditions.

### 3. Model of BESS with voltage support capability

As mentioned in the introduction, the proposed TNEP model improves system dynamic performance during contingencies by increasing system strength in weak network areas. For this, the BESS control includes an additional control loop to inject reactive current during voltage dips. The general block diagram of the control scheme used is shown in Fig. 1.

The voltage support capability of the BESS is implemented in block “ $i_q$  during contingencies”. This control loop is activated if the voltage deviation at the point of common coupling (PCC) is such that  $|\Delta V_{PCC}| \geq 10\%$ . In this case, the reference of the reactive current to be injected by the BESS ( $i_q^{ref}$ ) is calculated according to:

$$i_q^{ref} = K|\Delta V_{PCC}|i_n \text{ if } |\Delta V_{PCC}| \geq 10\% \quad (1)$$

where  $i_n$  is the BESS nominal current and  $K$  the slope of the line characterizing reactive current injection during failures ( $K \geq 2$ ) [27]. If  $|\Delta V_{PCC}| < 10\%$ , the system is in normal operation and the BESS operates with power factor control (block “ $i_q$  in steady state”). To avoid exceeding the current limits of the converter during severe voltage dips, a current limiter is added for limiting  $i_d^{ref}$  according to:

$$i_d^{ref} \leq \sqrt{1.2^2 - (i_q^{ref})^2} \quad (2)$$

### 4. Proposed TNEP model including strength constraints

#### 4.1. Overview

The proposed TNEP determines the optimal expansion plan optimizing additional transmission network capacity and BESS, while satisfying a set of strength constraints. These constraints are formulated based on a logistic regression model that exploits the relationship between the SCLs and system stability during faults. The optimization problem is solved iteratively in a two-stage algorithmic process, which is first based on an economic criterion and then on strength requirements.

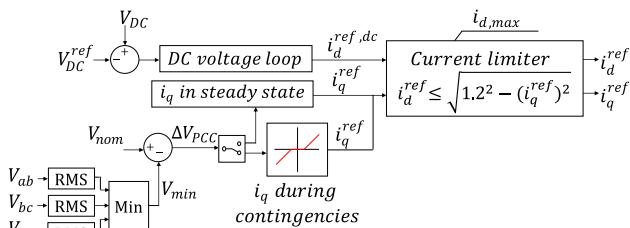


Fig. 1. BESS control scheme for voltage support during contingencies.

On the first stage, the optimal investment plan for transmission lines and BESS equipment is identified by a traditional cost minimization strategy [22]. Once the optimal expansion plan  $\bar{x}_j^*$  (iteration  $j$ ) and thus the new network setup is completed, the second stage assesses whether the expansion plan obtained in the previous stage complies with the strength constraints. If one of the strength constraints is not met, a new linear constraint (or “cut”) is generated and added to the first stage to remove that investment plan from the search space. Then, Stage 1 is performed again, yet in a limited search space. The iterative process described above continues until an optimal expansion plan  $\bar{X}^*$  fulfilling all strength constraints is found. The diagram in Fig. 2 shows the iterative process associated with the proposed TNEP model. Importantly, second stage constraints represent the probability of the system remaining stable after a major fault, which is formulated by using logistic regressions over offline simulation results that relate the SCLs and the stable/unstable statuses of the system after a fault. To determine whether a short-circuit simulation is stable or not, the angular, frequency and voltage stability in the system are observed. If any of these are unstable, the whole simulation is determined to be unstable as suggested in [28].

Remarkably, the first stage corresponds to a traditional mathematical program that optimizes transmission expansion plans and energy storage facilities. Hence, the key modeling contribution of this work is twofold. First, the unique characteristic of the algorithmic process to generate new linear constraints that can be added in the first stage to remove solutions that do not meet the strength requirements. And second, the formulation of second stage’s constraints via logistic regressions over simulation results relating SCLs and stable/unstable statuses of the system after a fault. In the following subsections, the details of both stages are presented.

#### 4.2. Stage 1

The TNEP model used in this stage can be a traditional transmission expansion program. For example, we choose to use a deterministic model that includes an evaluation horizon of one year—subjected to the classical technical constraints used in planning studies [15,29]. The technical constraints are related to the operational limits of generation units, load balance, and transmission capacity [22]. The optimization minimizes the total costs of the system by including operational and investment costs, as well as the energy not supplied. We consider time-coupling constraints to capture the effects of BESS as in [30].

#### 4.3. Stage 2

##### 4.3.1. Set of strength constraints

The TNEP model includes a set of  $nb$  strength constraints, one constraint for each network busbar, where  $nb$  is the number of busbars in the network. To formulate the constraints, a set of probability cumulative distribution functions  $p_b(SCL_b)$  is used, so that  $b \in \{1, 2, \dots, k, \dots, nb\}$ . For busbar  $b$ , with a short-circuit level of  $SCL_b$ , function  $p_b(SCL_b)$  yields the probability that the system is stable in case of a three-phase short circuit in busbar  $b$ .

To formulate strength requirements, let  $SL^*$  be the security level—in terms of stability—required by the system planner. In such case, the optimal expansion plan will be that which, for any three-phase short-

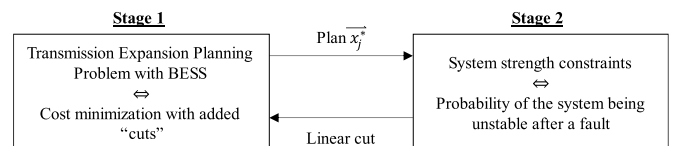


Fig. 2. Overview of proposed TNEP model.

circuit happening in a busbar in the system  $b \in \{1, 2, \dots, nb\}$ , satisfies that the probability of the system being stable is greater than or equal to  $SL^*$ . Note  $SL^*$  can be understood as a probability threshold, indicating the minimum requirement over the chances of the system to remain stable under a fault. This way, if  $\vec{x}_j^*$  is the expansion plan obtained in iteration  $j$  in Stage 1, the set of  $nb$  stability constraints to be considered in Stage 2 (for said iteration) will be:

$$p_b \left( SCL_b \left( \vec{x}_j^* \right) \right) \geq SL^* \forall b \in \{1, 2, \dots, nb\}, \quad (3)$$

where  $SCL_b \left( \vec{x}_j^* \right)$  is a function that estimates the value of the SCL at busbar  $b$  given an expansion plan  $\vec{x}_j^*$ . Function  $SCL_b \left( \vec{x}_j^* \right)$  uses Thevenin equivalent ( $Z_{th}^b$ ) seen in each busbar  $b$  of the grid, by considering system parameters, such as transmission line impedances and SGs transient reactance [8]. Additionally, the calculation of the SCL considers that BESS and CIG have voltage support capability, i.e., they inject reactive current during short circuits. The support is, however, limited to 1.1 times their rated current due to the thermal limits of the converters. Once the  $Z_{th}^b$  is obtained, the short-circuit power is calculated as  $Z_{th}^{b-1}$ , considering a voltage of 1.0 [p.u] for each busbar.

If the expansion plan obtained in iteration  $j$  ( $\vec{x}_j^*$ ) meets all constraints defined in (3), then plan  $\vec{x}_j^*$  is the optimal plan  $\vec{x}^*$  and the optimization process ends. On the contrary, if one or more of the constraints defined in (3) are not met, plan  $\vec{x}_j^*$  is removed from the search space by incorporating a supplementary linear constraint in Stage 1. Then,  $j = j + 1$ , and Stage 1 is performed again, but now considering a limited search space due to the extra linear constraint (or cut).

#### 4.3.2. Determination of cumulative distribution functions

Functions  $p_b(\cdot)$  in (3) relate the probability that the system is stable in case of a three-phase short circuit with the SCLs of the network at busbar  $b$ . These functions are built based on a logistic regression model that exploits the relationship between the SCLs and the dynamic performance of the system during faults. Considering that different types of grid busbars have different characteristics in terms of strength, the cumulative distribution functions are calculated for 3 types of busbars: generation, load, and HV-transmission.

To formulate the logistic regression model, a dataset should first be generated to establish the relationship between SCLs and system dynamic response. For this, we use a simulation-based approach considering time domain simulations. To cover a wide spectrum of scenarios, the simulation process must include several operating points and contingencies in several busbars distributed throughout the grid. The simulated faults are three-phase short circuits cleared by opening the pertinent line circuit.

To establish the relationship between the SCLs and the stability of the system, the matrix  $\mathcal{R}^m$  is defined for each simulation of an operating point  $m$ . To determine matrix  $\mathcal{R}^m$ , in each simulation, the following is logged: (i) the SCL of the busbar in which the fault occurs and (ii) "1" if the system is stable or "0" if it is not (because of this binary outcome we use a logistic regression). Eq. (4) illustrates  $\mathcal{R}^m$  for the system operation point  $m$ .

$$\mathcal{R}^m = \begin{pmatrix} (SCL_1^m, 1 \text{ or } 0) \\ \vdots \\ (SCL_k^m, 1 \text{ or } 0) \\ \vdots \\ (SCL_{nb}^m, 1 \text{ or } 0) \end{pmatrix}. \quad (4)$$

From the dataset  $(SCL_k^m, 1 \text{ or } 0)$  for a given type of busbar (data

corresponding to an  $\mathcal{R}^m$  subset), it is possible to obtain a sigmoid curve. This curve describes the relation between the probability that the system is stable during a short circuit in busbar  $b$  with  $SCL_b$ . These probabilities are modeled properly by means of curves as follow [31]:

$$p(x) = \frac{1}{1 + e^{-(\beta_0 + \beta_1 x)}} \quad (5)$$

where  $p(x)$  is the function of probability cumulative distribution functions,  $x$  is the independent variable, and  $\beta_0$  and  $\beta_1$  are coefficients which characterize the curve determined from certain input data by using the logistic regression technique [31]. Fig. 3 shows the sigmoid curve (5) obtained in the case of a load busbar. The blue dots are the data  $(SCL_k^m, 1 \text{ or } 0)$  obtained in the dynamic simulations for the different operation points  $m$ . For example, the green dot in the figure (1300, 0.89) means that if there is a short circuit near load busbar with a SCL of 1300 MVA, the probability that the system is stable is 89%. In fact, the higher the SCL in the busbar, the greater the probability that the system will remain stable after a short circuit.

#### 4.3.3. Generation of linear constraints or "cuts"

As mentioned earlier, if one of the strength constraints in (3) is not met by the investment plan  $\vec{x}_j^*$ , a linear constraint is defined to eliminate that solution of the search space in the first stage. For this, let  $\vec{x}^*$  be the optimal solution from the last iteration or point of the investment plan that must be removed. To cut this point from the search space, we can write:

$$\sum_{i \in A} x_i + \sum_{j \in B} (1 - x_j) \leq n - 1, \quad (6)$$

where  $\vec{x} = (x_1, x_2, \dots, x_i)$  represents the vector of binary decision variables in the new iteration,  $A$  is the set of indices with ones in  $\vec{x}^*$  (solution of the last iteration) that will be cut from the search space,  $B$  is the set of indices with zeros in  $\vec{x}^*$ , and  $n$  is the cardinality or length of  $\vec{x}^*$ . Note that this constraint will only remove  $\vec{x}^*$  from the search space.

This constraint is sent to Stage 1 each time the solution  $\vec{x}^*$  found does not meet the stability requirements defined in (3). This way, the economic problem is solved again, but without considering the solution discarded in Stage 2.

## 5. Case study

The network used to test the proposed TNEP model corresponds to a reduced version of the Northern Interconnected System of Chile (NIS) of the year 2021. The model includes 20 busbars and 23 transmission lines at 220 kV (14 double circuit and 9 single circuit lines). The generation mix is composed of 45 SGs and 21 CIG-based power plants distributed in different network busbars. The installed capacity of photovoltaic and wind power is 3580 MW and 1350 MW, respectively, which translates into 27% CIG penetration of the total installed capacity of the system.

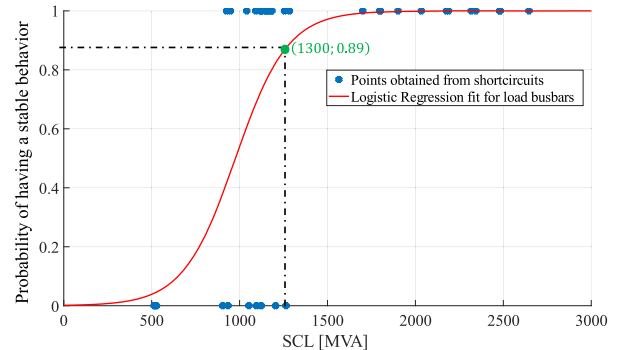


Fig. 3. Sigmoid curve for load busbars.

The system demand throughout the year is approximately constant with a peak value of 3022 MW. We use Gurobi 9.1.2.

Fig. 4 shows the one-line diagram of the NIS. Red lines represent candidate circuits for transmission expansion, while blue bars illustrate candidate busbars to install BESS.

Fig. 5 summarizes the analyzed scenarios. Two cases are included for planning: where  $case_{BESS}^{87\%}$  (with strength constraints), for example, denotes that the probability that the system is stable during a short circuit must be  $SL^* \geq 87\%$  (security level  $\geq 87\%$ ). In addition, the analysis includes two base cases:  $case_0^{Base}$ , which includes a traditional TNEP without strength constraints and without BESS, and  $case_{BESS}^{Base}$ , which includes a traditional TNEP without strength constraints while including BESS.

The model is executed for the year 2021, allowing for up to five BESS modules per candidate busbar, with each BESS module having a capacity of 50 MW. All pertinent data, including costs, as well as generation and demand profiles, have been derived and adapted from the context of Chile, as documented in [32]. Regarding the sigmoid curves used, Fig. 6 shows the curves obtained following the logistic regression technique presented in Section IV. The curves show the probability that the power system is stable during a short circuit as a function of the SCL of each type of grid busbar. As expected, the figure reveals that the curves obtained for both HV-transmission and load busbars are relatively similar, whereas the curves for generation busbars show more distinct differences.

### 6. Results

Table 1 shows the results obtained with the proposed TNEP considering BESS for different security levels ( $SL^*$ ). Operation costs, investment costs, and total costs in millions of dollars (MMUSD) are included for all case studies.

Table 1 shows that when the planning includes BESS devices, the total cost of the system remains relatively constant, regardless of the security level  $SL^*$  required. This is observed when comparing the total costs of the case without strength constraints ( $case_{BESS}^{Base}$ ; 836.0 MMUSD), with the costs of case  $SL^* = 93\%$  ( $case_{BESS}^{93\%}$ , 838.1 MMUSD). The comparison shows that the increase in the total costs due to the strength requirements is marginal (0.24 %). This proves that reinforcing weak areas of the network for improving system dynamic performance during contingencies does not imply a significant penalty in economic terms, at least not when it comes to total costs. It is worth mentioning that the

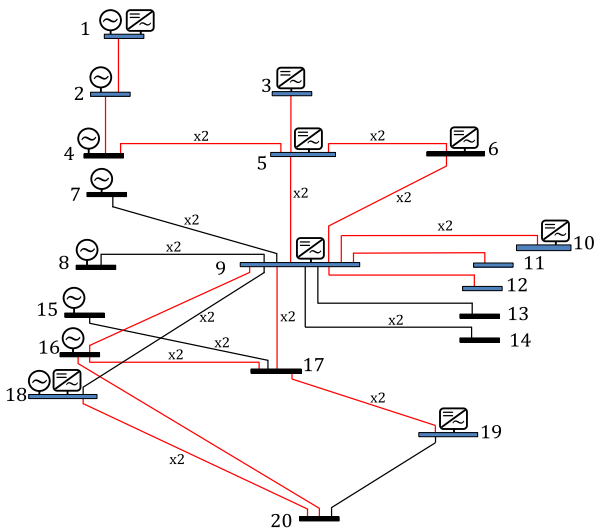


Fig. 4. Simplified NIS including candidate line circuits and candidate busbars to install BESS.

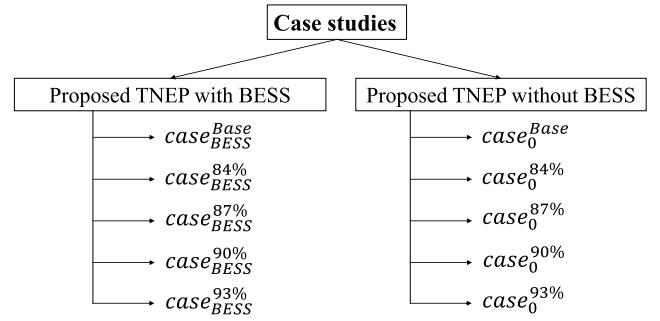


Fig. 5. Scenarios under study.

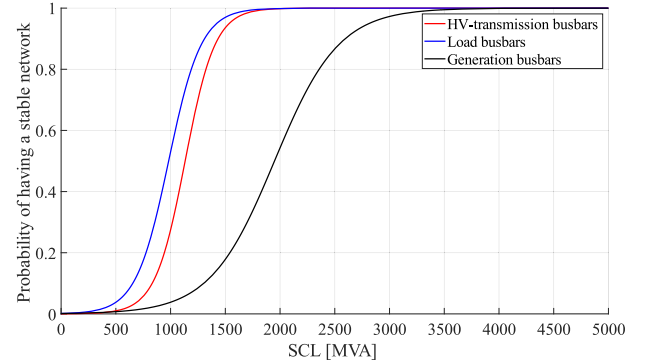


Fig. 6. Sigmoid curves according to type of busbar.

Table 1

Summary of obtained results. Case TNEP with BESS.

Costs [MMUSD]	$case_{BESS}^{Base}$	$case_{BESS}^{84\%}$	$case_{BESS}^{87\%}$	$case_{BESS}^{90\%}$	$case_{BESS}^{93\%}$
Investment costs	9.8	19.8	24.1	24.6	25.8
Operation costs	826.2	816.2	812.6	812.9	812.3
<b>Total costs</b>	<b>836.0</b>	<b>836.0</b>	<b>836.7</b>	<b>837.5</b>	<b>838.1</b>

increase in the total costs is accompanied by a higher security level associated with a lower probability of energy not supplied and blackout events, benefits that are not explicitly acknowledged in the optimization. Unfortunately, the costs of power interruptions in real electricity systems are extremely difficult to quantify or estimate, so they are usually not explicitly considered in the planning stage. Despite this, these benefits could counteract the cost increase observed in Table 1.

Table 2 shows the same results as Table 1, but for the planning case without BESS.

When comparing Tables 1 and 2, it can be seen that although incorporating BESS devices into the planning always leads to a significant increase in investment costs, it also produces a considerable reduction in operating costs. The net result of both effects is that by including BESS, the total costs of the system decrease, regardless of the level of security required.

Tables 3 and 4 show the planning results obtained in terms of BESS devices and line circuits that were installed in each case. Table 3 shows

Table 2

Summary of obtained results. Case TNEP without BESS.

Costs [MMUSD]	$case_0^{Base}$	$case_0^{84\%}$	$case_0^{87\%}$	$case_0^{90\%}$	$case_0^{93\%}$
Investment costs	7.3	4.3	4.3	5.7	7.0
Operation costs	834.3	857.7	857.7	857.7	857.8
<b>Total costs</b>	<b>841.6</b>	<b>862.0</b>	<b>862.0</b>	<b>863.4</b>	<b>864.8</b>

**Table 3**

Total installed BESS modules and line circuits. Case TNEP with BESS.

Element	case <sub>BESS</sub> <sup>Base</sup>	case <sub>BESS</sub> <sup>84%</sup>	case <sub>BESS</sub> <sup>87%</sup>	case <sub>BESS</sub> <sup>90%</sup>	case <sub>BESS</sub> <sup>93%</sup>
BESS	2	4	5	5	5
Line circuit	1	3	3	4	5

**Table 4**

Total installed line circuits. Case TNEP without BESS.

Element	case <sub>0</sub> <sup>Base</sup>	case <sub>0</sub> <sup>84%</sup>	case <sub>0</sub> <sup>87%</sup>	case <sub>0</sub> <sup>90%</sup>	case <sub>0</sub> <sup>93%</sup>
Line circuit	4	5	5	7	8

the total number of BESS modules and line circuits installed in the case of the proposed TNEP including BESS. Table 4 shows the same information in the case where planning does not consider BESS.

When the planning considers BESS, the results show that as the strength constraints become more stringent (higher  $SL^*$ ), the optimization model tends to install more line circuits and/or BESS equipment in the less robust areas of the system. This is the case of the weak busbars {1, 2, 3, 4, 5} and {10, 11, 12} (see Fig. 4), all of them characterized by low SCLs. In fact, while in the base case with BESS (case<sub>BESS</sub><sup>Base</sup>), 2 BESS and only 1 line circuit are installed, in the case  $SL^* = 93\%$ , a total of 5 line-circuits and 5 BESS modules must be installed (see Table 3).

On the other hand, the results show that when the planning does not include BESS equipment, increasing the  $SL^*$  also leads to mesh more the weak areas of the network. However, since in this case the planning only includes new line circuits, the result is less efficient compared to the case in which BESS are considered. In fact, even in the least demanding case in terms of security (case<sub>0</sub><sup>84%</sup>), 5 additional line circuits are installed, while in case  $SL^* = 93\%$ , 8 line-circuits are installed. What is more, Table 4 shows that in cases  $SL^* = 84\%$  and  $SL^* = 87\%$ , the same expansion plan is obtained (5 additional line circuits) despite having different strength requirements. This reflects an inefficiency in the case  $SL^* = 84\%$ , since the optimal plan in that case raises the SCLs to values higher than the minimum required.

To see the dynamic validation of the above plans, the readers are addressed to the Online Appendix [33].

## 7. Conclusions

We introduce a transmission expansion planning model that incorporates system strength constraints quantified through SCL. This model optimally determines network expansions, including battery systems, in light of the rising penetration of converter interfaced generation. Using a master-slave algorithm to solve the introduced planning problem, we identify various investment strategies that incorporate additional circuits and/or battery equipment, tailored to specific security levels (strength requirements). Importantly, our findings indicate that a transmission plan employing simplified stability criteria via strength constraints can substantially enhance a power system's dynamic response during short circuits. As security requirements intensify, there's a discernible trend towards improved system dynamics during short circuits. While the integration of battery devices into planning does escalate initial investment costs, the consequent reduction in operational expenses plus the contribution towards the stipulated security level (strength requirements), invariably lead to overall cost savings.

Dynamic validation of the proposed investment strategies underscores the enhanced dynamic system performance during faults when an optimal mix of battery and new lines is prioritized. This emphasizes the imperative of factoring in battery systems in future transmission expansion strategies. Crucially, these battery systems should encompass a reactive current injection control to truly bolster system stability during faults.

## CRedit authorship contribution statement

**Juan Pablo Cerda:** Conceptualization, Data curation, Formal analysis, Methodology, Writing – original draft. **Claudia Rahmann:** Supervision, Writing – original draft, Writing – review & editing, Conceptualization, Formal analysis, Funding acquisition. **Rodrigo Moreno:** Formal analysis, Funding acquisition, Methodology, Supervision, Writing – original draft, Writing – review & editing. **Luis Morán:** Formal analysis, Funding acquisition, Methodology, Supervision, Writing – original draft, Writing – review & editing.

## Declaration of competing interest

The authors declare that they have no known competing financial interests or personal relationships that could have appeared to influence the work reported in this paper.

## Data availability

Data will be made available on request.

## Acknowledgments

This work was funded by ANID, Chile through grants PIA/PUENTE AFB230002 (ISCI), FONDECYT 1231924, Fondap/1523A0006 (SERC-Chile) and BASAL/FB0008 (AC3E).

## References

- [1] IRENA. Renewable energy statistics 2023, International Renewable Energy Agency, Abu Dhabi, 2023. [https://mc-cd8320d4-36a1-40ac-83cc-3389-cdn-endpoint.azureedge.net/-/media/Files/IRENA/Agency/Publication/2023/Jul/IRENA\\_Renewable\\_energy\\_statistics\\_2023.pdf?rev=7b2f44c294b84cad9a27fc24949d2134](https://mc-cd8320d4-36a1-40ac-83cc-3389-cdn-endpoint.azureedge.net/-/media/Files/IRENA/Agency/Publication/2023/Jul/IRENA_Renewable_energy_statistics_2023.pdf?rev=7b2f44c294b84cad9a27fc24949d2134).
- [2] IEEE/NERC Task Force on Short-Circuit and System Performance Impact of Inverter Based Generation, Impact of inverter based generation on bulk power system dynamics and short-circuit performance, IEEE Power Energy Soc. (2018).
- [3] North American Electric Reliability Corporation (NERC), "Integrating inverter based resources into weak power systems," Reliability Guideline, June 2017.
- [4] North American Electric Reliability Corporation (NERC), "Short-Circuit Modelling and System Strength," White Paper, February 2018.
- [5] S. Huang, J. Schmall, J. Conto, J. Adams, Y. Zhang, C. Carter, Voltage control challenges on weak grids with high penetration of wind generation: ERCOT experience, in: 2012 IEEE Power and Energy Society General Meeting, 2012, pp. 1–7.
- [6] M. Gomes, R. Sharma, F. Martin, Pramod Ghimire, G. Yang, Concerning short-circuit current contribution challenges of large-scale full-converter based wind power plants, IEEE Access. 11 (Jan. 2023) 64141–64159.
- [7] B. Kroposki, B. Johnson, Y. Zhang, V. Gevorgian, P. Denholm, B. Hodge, B. Hannegan, Achieving a 100% renewable grid: operating electric power systems with extremely high levels of variable renewable energy, IEEE Power Energy Mag. 15 (2017).
- [8] N. Tleis, Power Systems Modelling and Fault analysis: Theory and Practice, Elsevier, 2007.
- [9] L. Fan, Z. Miao, An explanation of oscillations due to wind power plants weak grid interconnection, IEEE Trans. Sustain. Energy 9 (1) (2018) 488–490.
- [10] J. Machowski, P. Kacejko, S. Robak, P. Miller, M. Wanczer, Simplified angle and voltage stability criteria for power system planning based on the short-circuit power, Int. Trans. Electr. Energy Syst. 25 (11) (2015) 3096–3108.
- [11] J. Machowski, J. Bialek, J. Bumby, Power System Dynamics: Stability and Control, 2nd Edition, John Wiley & Sons, 2008.
- [12] A. Kanchanaharuthai, V. Chankong, K.A. Loparo, Transient stability and voltage regulation in multimachine power systems vis-à-vis STATCOM and battery energy storage, IEEE Trans. Power Syst. 30 (5) (2015) 2404–2416.
- [13] A. Jalali, M. Aldeen, Short-term voltage stability improvement via dynamic voltage support capability of ESS devices, IEEE Syst. J. 13 (4) (Dec. 2019) 4169–4180.
- [14] I. Erlich, F. Shewarega, S. Engelhardt, J. Kretschmann, J. Fortmann, F. Koch, Effect of wind turbine output current during faults on grid voltage and the transient stability of wind parks, IEEE Power Energy Soc. Gen. Meet. (2009) 1–8.
- [15] D.S. Kirschen, G. Strbac, Fundamentals of Power System Economics, Wiley Online Library, 2004.
- [16] T. Ngo, M. Lwin, S. Santoso, Power transmission expansion planning based on voltage stability indexes, in: 2017 IEEE Power & Energy Society General Meeting, 2017, pp. 1–4.
- [17] H. Karimianfard, H. Haghghat, B. Zeng, Co-optimization of battery storage investment and grid expansion in integrated energy systems, IEEE Syst. J. 16 (4) (Dec. 2022) 5928–5938.

- [18] C.E. Okafor, K.A. Folly, Provision of additional inertia support for a power system network using battery energy storage system, *IEEE Access*. 11 (Jan. 2023) 74936–74952.
- [19] H. Golpira, A. Atarodi, S. Amini, A.R. Messina, B. Francois, H. Bevrani, Optimal energy storage system-based virtual inertia placement: a frequency stability point of view, *IEEE Trans. Power Syst.* 35 (6) (Nov. 2020) 4824–4835.
- [20] M. Alanazi, M. Salem, Mohammad Hosein Sabzalian, Natarajan Prabakaran, S. Ueda, Tomonobu Senjyu, Designing a new controller in the operation of the hybrid PV-BESS system to improve the transient stability, *IEEE Access*. 11 (Jan. 2023) 97625–97640.
- [21] N. Cifuentes, C. Rahmann, F. Valencia, R. Alvarez, Network allocation of bess with voltage support capability for improving the stability of power systems, *IET Gener. Transm. Distrib.* (2019).
- [22] G. Pulazza, N. Zhang, C. Kang, C.A. Nucci, Transmission planning with battery-based energy storage transportation for power systems with high penetration of renewable energy, *IEEE Trans. Power Syst.* 36 (6) (Nov. 2021) 4928–4940.
- [23] T. Qiu, B. Xu, Y. Wang, Y. Dvorkin, D.S. Kirschen, Stochastic multistage coplanning of transmission expansion and energy storage, *IEEE Trans. Power Syst.* 32 (1) (2017) 643–651.
- [24] S. Teimourzadeh, F. Aminifar, MILP formulation for transmission expansion planning with short-circuit level constraints, *IEEE Trans. Power Syst.* 31 (4) (Jul. 2016) 3109–3118.
- [25] H. Gharibpour, F. Aminifar, M. Haji Bashi, Short-circuit-constrained transmission expansion planning with bus splitting flexibility, *IET Gener. Transm. Distrib.* 12 (1) (Nov. 2017) 217–226.
- [26] M. Esmaili, M. Ghamsari-Yazdel, N. Amjadi, A.J. Conejo, Short-circuit constrained power system expansion planning considering bundling and voltage levels of lines, *IEEE Trans. Power Syst.* 35 (1) (Jan. 2020) 584–593.
- [27] VDE, “Technical connection rules for extra-high voltage (VDE-AR-N 4130),” 2018.
- [28] N. Hatziaargyriou, J. Milanovic, C. Rahmann, V. Ajjarapu, C. Canizares, I. Erlich, ... & C. Vournas, Definition and classification of power system stability–revisited & extended, *IEEE Trans. Power Syst.* 36 (4) (2020) 3271–3281.
- [29] R. Hemmati, R. Hooshmand, A. Khodabakhshian, Comprehensive review of generation and transmission expansion planning, *IET Gener. Transm. Distrib.* 7 (9) (2013) 955–964.
- [30] R. Moreno, A. Street, J.M. Arroyo, P. Mancarella, Planning low-carbon electricity systems under uncertainty considering operational flexibility and smart grid technologies, *Phil. Trans. R. Soc. A: Math. Phys. Eng. Sci.* 375 (2100) (2017) 20160305.
- [31] S. Menard, *Logistic regression: From Introductory to Advanced Concepts and Applications*, Sage, 2010.
- [32] A. Inzunza, F.D. Muñoz, R. Moreno, Measuring the effects of environmental policies on electricity markets risk, *Energy Econ.* 102 (2021) 105470.
- [33] J.P. Cerda, C. Rahmann, R. Moreno, L. Moran, 2024 Co-optimizing transmission and BESS expansions with system strength constraints, Online Appendix, URL: <http://bit.ly/pssc24apdx>.